

High-Yield Two-Dimensional CdS Nanowire Networks Synthesized by a Low-Temperature Chemical Method

Haiyan Li and Jun Jiao*

Department of Physics, Portland State University, P.O. Box 751, Portland, Oregon 97207

Received March 27, 2008

We report here on a one-step chemical procedure for the synthesis of monolayer and multilayer CdS square grid planar nanowire networks (SGP-NWNs). This procedure utilizes a chelation–deposition–epitaxy (CDE) mechanism to convert $\text{Cd}(\text{CH}_3\text{COO})_2 \cdot 2\text{H}_2\text{O}/\text{S}/\text{C}_{32}\text{H}_{66}$ through the multilayer structures of bismuth triiodide (BiI_3) flakes to CdS SGP-NWNs. In the CDE synthesis, ordered pyramid-shaped nanoparticles and SGP-NWNs were formed at 160 and 185 °C, respectively. TEM and SEM characterizations indicate that the SGP networks consist of interconnected CdS single-crystalline nanowires. A systematic investigation of the correlation between the preparation conditions and the morphologies of the nanostructures suggests that the formation of SGP-NWNs is attributed to the electrostatic force between the Bi–I bonds and Cd cations acting on the CdS nanowire isotropic crystalline growth. Further experimentation demonstrates that using BiI_3 flake and CDE procedures similar to nanowire networks of different chemical compositions can be synthesized on a variety of substrates.

Introduction

In the last several years, research using one-dimensional (1D) nanowires and nanotubes to fabricate nanodevices has demonstrated their advantages in applications^{1,2} including transistors,³ nano biosensors,⁴ nano lasers,⁵ solar cells,⁶ and nano generators.⁷ However, these nanodevices were fabricated with either a single nanowire in an isolated case or with a nanowire array which requires complicated, multistep nanofabrication processes to assemble.^{8–10} To utilize nanostructure-based devices for practical applications, it is imperative to develop an effective method for mass production that guarantees uniform structural, compositional, electronic, and optical properties. In the context of nanodevice fabrication, theoretical studies have suggested that when 1D nanostructures are connected covalently, they are expected to possess mechanical, electronic, and porosity properties that are strikingly different from those of isolated 1D building blocks.¹¹

The ability to tailor nanostructures into networks is the foundation for the mass production of nano- and microde-

vices with controlled properties. To date, little is known regarding the different ways nanowire networks can be created and how the architecture configuration affects the nanowires' physical and chemical properties. Recently, several groups reported the synthesis of uniform three-dimensional (3D) tungsten oxide nanowire networks,¹² PbSe 3D nanowire networks,¹³ and interconnected InAs nanowire networks formed with InAs nanotree structures.¹⁴ All these structures were prepared by thermal evaporation and deposition at high temperatures which are not favorable methods for device integrations. Although a few efforts have been made using low-temperature chemical routes to fabricate nanowire networks, the structure varies broadly depending on the method used. Ramanath et al. synthesized randomly ordered two-dimensional (2D) and 3D networks of gold nanowires by agitating nanoparticles in a toluene–aqueous mixture,¹⁵ while Wang et al. prepared metal and semiconductor nanowire network thin films using pore structures as a template by electrochemical processes.¹⁶ The common drawback introduced by these processes is the poor crystallinity and uniformity in the network structures. Further, Sigman and Korgel observed the growth of Bi_2S_3 nanofabrics induced by heterogeneous nanowire nucleation and epitaxial elongation from the surface of existing wires.¹⁷ However, the yield of this nanostructure is rather low.

* Corresponding author. E-mail: jiao@pdx.edu.

- (1) Law, M.; Goldberger, J.; Yang, P. *Annu. Rev. Mater. Sci.* **2004**, *34*, 83.
- (2) Lieber, C. M.; Wang, Z. L. *MRS Bull.* **2007**, *32*, 99.
- (3) Xiang, J.; Lu, W.; Hu, Y.; Wu, Y.; Yan, H.; Lieber, C. M. *Nature* **2006**, *441*, 489.
- (4) Patolsky, F.; Zheng, G.; Lieber, C. M. *Nat. Protocols* **2006**, *1*, 1711.
- (5) Huang, M. H.; Mao, S.; Feick, H.; Yan, H. Q.; Wu, Y. Y.; Kind, H.; Weber, E.; Russo, R.; Yang, P. D. *Science* **2001**, *292*, 1897.
- (6) Huynh, W. U.; Dittmer, J. J.; Alivisatos, A. P. *Science* **2002**, *295*, 2425.
- (7) Wang, Z. L.; Song, J. H. *Science* **2006**, *312*, 242.
- (8) Agarwal, R.; Ladavac, K.; Roichman, Y.; Yu, G. H.; Lieber, C. M.; Grier, D. G. *Opt. Express* **2005**, *13*, 8906.
- (9) Beckman, R.; Johnston-Halperin, E.; Luo, Y.; Green, J. E.; Heath, J. R. *Science* **2005**, *310*, 465.
- (10) Ahn, J. H.; Kim, H. S.; Lee, K. J.; Jeon, S.; Kang, S. J.; Sun, Y. G.; Nuzzo, R. G.; Rogers, J. A. *Science* **2006**, *314*, 1754.
- (11) Romo-Herrera, J. M.; Terrones, M.; Terrones, H.; Dag, S.; Meunier, V. *Nano Lett.* **2007**, *7*, 570.

- (12) Zhou, J.; Ding, Y.; Deng, S. Z.; Gong, L.; Xu, N. S.; Wang, Z. L. *Adv. Mater.* **2005**, *17*, 2107.
- (13) Zhu, J.; Peng, H.; Chan, C. K.; Jarausch, K.; Zhang, X. F.; Cui, Y. *Nano Lett.* **2007**, *7*, 1095.
- (14) Dick, K. A.; Deppert, K.; Karlsson, L. S.; Seifert, W.; Wallenberg, L. R.; Samuelson, L. *Nano Lett.* **2006**, *6*, 2842.
- (15) Ramanath, G.; D'Arcy-Gall, J.; Maddanimath, T.; Ellis, A. V.; Ganesan, P. G.; Goswami, R.; Kumar, A.; Vijayamohanan, K. *Langmuir* **2004**, *20*, 5583.
- (16) Wang, D.; Jakobson, H. P.; Kou, R.; Tang, J.; Fineman, R. Z.; Yu, D.; Lu, Y. *Chem. Mater.* **2006**, *18*, 4231.
- (17) Sigman, M. B.; Korgel, B. A. *Chem. Mater.* **2005**, *17*, 1655.

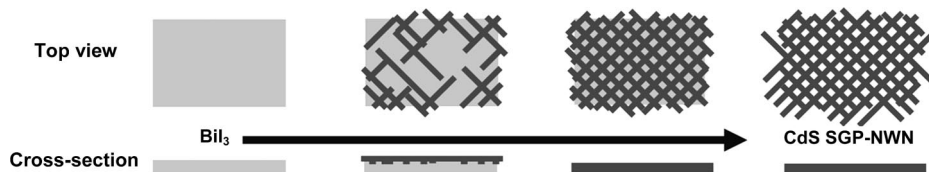


Figure 1. Schematic diagrams of the chelation–deposition–epitaxy growth process demonstrating the fabrication of the CdS SGP-NWNs with the assistance of the BiI_3 . Successive images illustrate the results of the reaction as a function of time.

In this report, we demonstrate a solution-phase synthesis of high-yield nanowire networks based on a chelation–deposition–epitaxy (CDE) growth mechanism that differs from either a solvent coordination molecular template (SCMT) mechanism¹⁸ or a solution–liquid–solid (SLS) mechanism.¹⁹ The CDE growth was conducted at the surface of a layered structure compound in a nonpolar organic solvent with long carbon atom chains. CdS ,^{20–22} one of the most important II–VI groups of semiconductors, was chosen to demonstrate the feasibility of the procedure. BiI_3 was selected as one of the preparation precursors due to its layered structure and polar Bi–I bonds aligned on its surface. A nonpolar organic solvent, $\text{C}_{32}\text{H}_{66}$, was used to provide a temperature-controlling reaction condition due to its high boiling point of 467 °C. Scanning electron microscope (SEM) and transmission electron microscope (TEM) characterizations of as-synthesized samples show that monolayer and multilayer CdS square grid planar nanowire networks (SGP-NWNs) with fine uniformity and high yield were formed. Figure 1 is a series of schematic diagrams that elucidates the formation process of a CdS SGP-NWN.

Experimental Section

Chemical and Substrate Preparation. Cadmium acetate dihydrate ($\text{Cd}(\text{CH}_3\text{COO})_2 \cdot 2\text{H}_2\text{O}$, 99.999%), sulfur powder (S, 99.5%), dotriacontane ($\text{C}_{32}\text{H}_{66}$, 97%), and bismuth(III) iodide (BiI_3 , 99.999%) were purchased from Alfa Aesar. Isopropanol and acetone were used as analytical reagents. Various types of substrates including Si, SiO_2/Si , and glass were ultrasonically cleaned in isopropanol and in acetone at room temperature and then dried with flowing nitrogen. A mixture of BiI_3 and ethanol was treated with an ultrasonicator for 20 min. The BiI_3 /ethanol supersaturated solution was prepared to allow the formation of BiI_3 flakes after 3 days. A pipet was used to transfer several drops of such solution onto the substrate to allow the BiI_3 flakes to be deposited on the surface of the substrate. The rest of the solution was stored for future use as the BiI_3 flakes can be preserved in the supersaturated solution.

Synthesis and Characterization of CdS SGP-NWNs. We mixed 0.2 g of $\text{Cd}(\text{Ac})_2 \cdot 2\text{H}_2\text{O}$ and 5 g of $\text{C}_{32}\text{H}_{66}$ into a reaction flask and heated it at 160 °C for 2 h. A substrate covered with BiI_3 flakes was immersed in the solution at 160–220 °C for 5 min. Then 0.15 g of S powder was added to the solution. The reaction time was kept at 3, 6, 12, 24, 36, and 48 h, respectively, for each sample. After the reaction, the substrate was retrieved from the solution. Residual $\text{C}_{32}\text{H}_{66}$ and unreacted chemicals on the surface of the

substrate were washed off using isopropanol at 60 °C and acetone at room temperature. The samples were then dried at 200 °C for 2 h.

The morphology and the internal structure of the CdS SGP-NWNs were analyzed using a FEI Sirion XL30 field emission SEM equipped with an energy-dispersive X-ray (EDX) spectrometer and a FEI Tecnai F-20 TEM equipped with a scanning transmission electron microscopy (STEM) capability and an EDX spectrometer.

Results and Discussion

Effect of Reaction Temperature on the Formation of CdS Nanostructures. Figure 2a shows an SEM image of the BiI_3 flakes deposited on a Si substrate before it was immersed into the reaction solution. Figure 2b–d displays the various morphologies formed on the substrate corresponding to different reaction temperatures. Note in Figure 2b that pyramid-shaped nanoparticles were formed on the surface of the flakes at 160 °C for 12 h. The bottom length of the quadrilateral plane ranges from 20 to 150 nm. Interestingly, most of the bottom lines of the pyramid-shaped nanoparticles are parallel to one another. The polygonal edges of the particles were mainly aligned in two intercrossed directions on the same flake. The particle distributions along the edges of the flakes were denser than those at the center of the flakes. When the reaction temperature was increased to 185 °C, typical monolayer SGP-NWNs were formed in which the nanowires align in two intercrossed directions and grow together in an interconnected configuration. Figure 2c is an SEM image demonstrating the structural configuration of a CdS SGP-NWN. The average diameter of the nanowires in a CdS SGP-NWN is 25–55 nm. The size of the SGP-NWN is dependent on the size of the BiI_3 flake. If the reaction temperature is higher than 220 °C, BiI_3 flakes decompose completely in 6 h and form Bi drops dispersed on the substrate and no CdS SGP-NWNs were observed as shown in Figure 2d.

We conducted annealing experiments on the samples to test the stability of the CdS SGP-NWNs. Our findings suggest that the samples synthesized at 185 °C with a reaction time longer than 24 h are stable under the annealing temperature of 200–300 °C for 2 h. Under this annealing condition no significant variations in the CdS SGP-NWNs were observed. However, the samples made at 185 °C with a reaction time of 12 h were not stable under the annealing temperatures of 250 and 300 °C. Note in Figure 3a, after the sample was annealed at 250 °C for 2 h, the SGP-NWNs started to agglomerate and were sintered into much thicker networks at an annealing temperature of 300 °C for 2 h (Figure 3b). This suggests that both reaction temperature and reaction time are important parameters for the quality of the SGP-NWNs.

(18) Wang, X.; Li, Y. D. *Inorg. Chem.* **2006**, *45*, 7522.

(19) Trentler, T. J.; Hickman, K. M.; Goel, S. C.; Viano, A. M.; Gibbons, P. C.; Buharo, W. E. *Science* **1995**, *270*, 1791.

(20) Peng, Z. A.; Peng, X. G. *J. Am. Chem. Soc.* **2001**, *123*, 183.

(21) Jun, J. Y.; Lee, S.; Kang, N.; Cheon, J. J. *Am. Chem. Soc.* **2001**, *123*, 5150.

(22) Dong, L. F.; Jiao, J.; Coulter, M.; Lover, L. *Chem. Phys. Lett.* **2003**, *376*, 653.

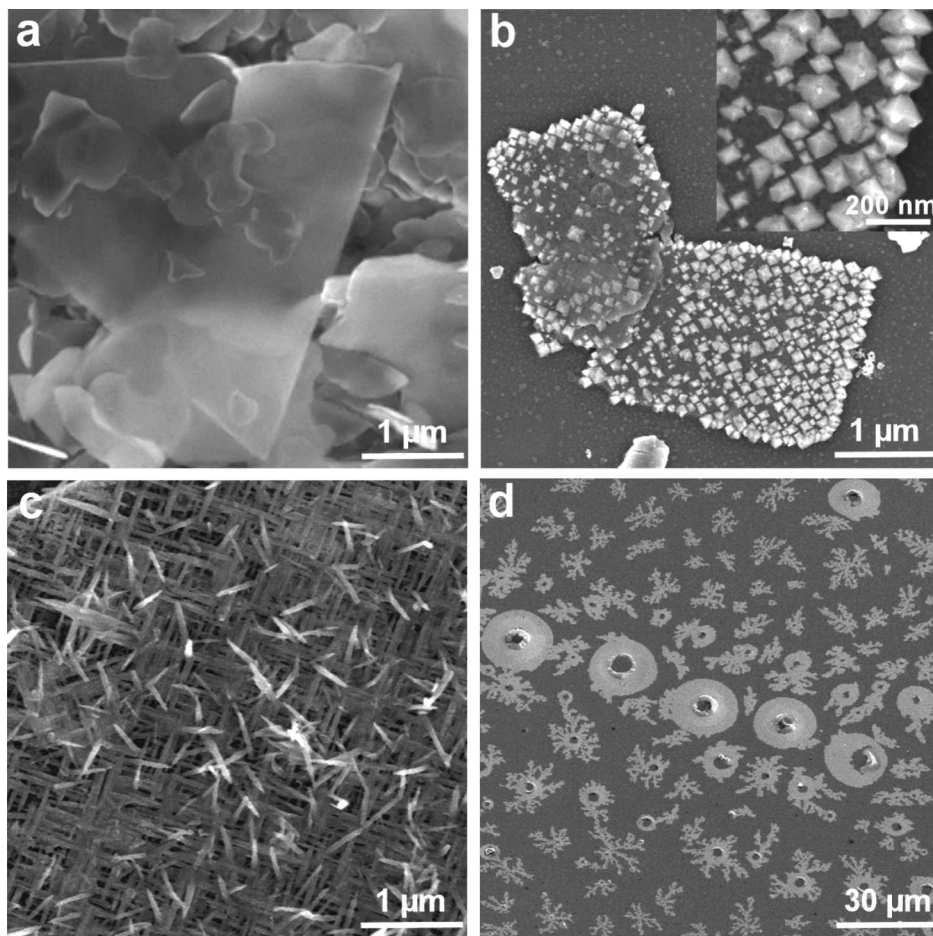


Figure 2. SEM images of (a) BiI_3 flakes; (b) ordered nanoparticles grown for 12 h at 160 °C; (c) monolayer SGP-NWNs grown for 12 h at 185 °C; (d) Bi drops obtained after 6 h of reaction at 220 °C.

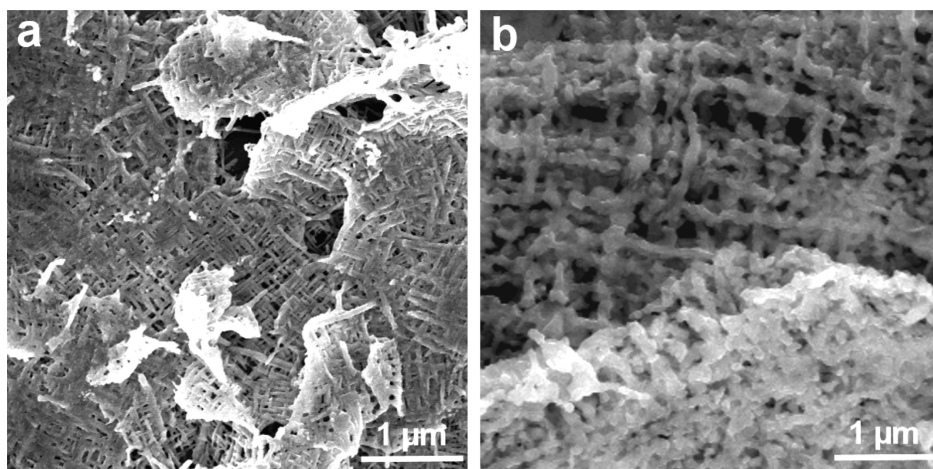


Figure 3. SEM images of SGP-NWNs grown at 185 °C for 12 h and annealed for 2 h at different temperatures: (a) 250 °C and (b) 300 °C, respectively.

Effect of Reaction Time on the Morphologies of the CdS Nanostructures. The reaction time not only has a significant impact on the stability of the SGP-NWN structures but also affects the morphology of the SGP-NWN formations. Figure 4a–f shows SEM images of six samples synthesized at 185 °C but with different reaction times. Figure 4a shows a sample with a reaction time of 3 h. Note that short CdS nanowires with a relatively low density distribution start to line up perpendicular to one another. Some nanowires connected to form T-shape nanostructures.

Only a few T-shape nanostructures were further connected to form small-size SGP-NWNs. All of the nanowires have a sharp tip on both ends and were aligned mainly in two intercrossed directions. It was noted that most of the nanowires were still associated with the BiI_3 flakes. As the reaction time increased to 6 h, larger areas of monolayer SGP-NWNs were formed by increasing connections among the nanowires on the flake as demonstrated in Figure 4b. The diameter of the nanowires is 30–40 nm. The density of the nanowires along the edge is slightly larger than that

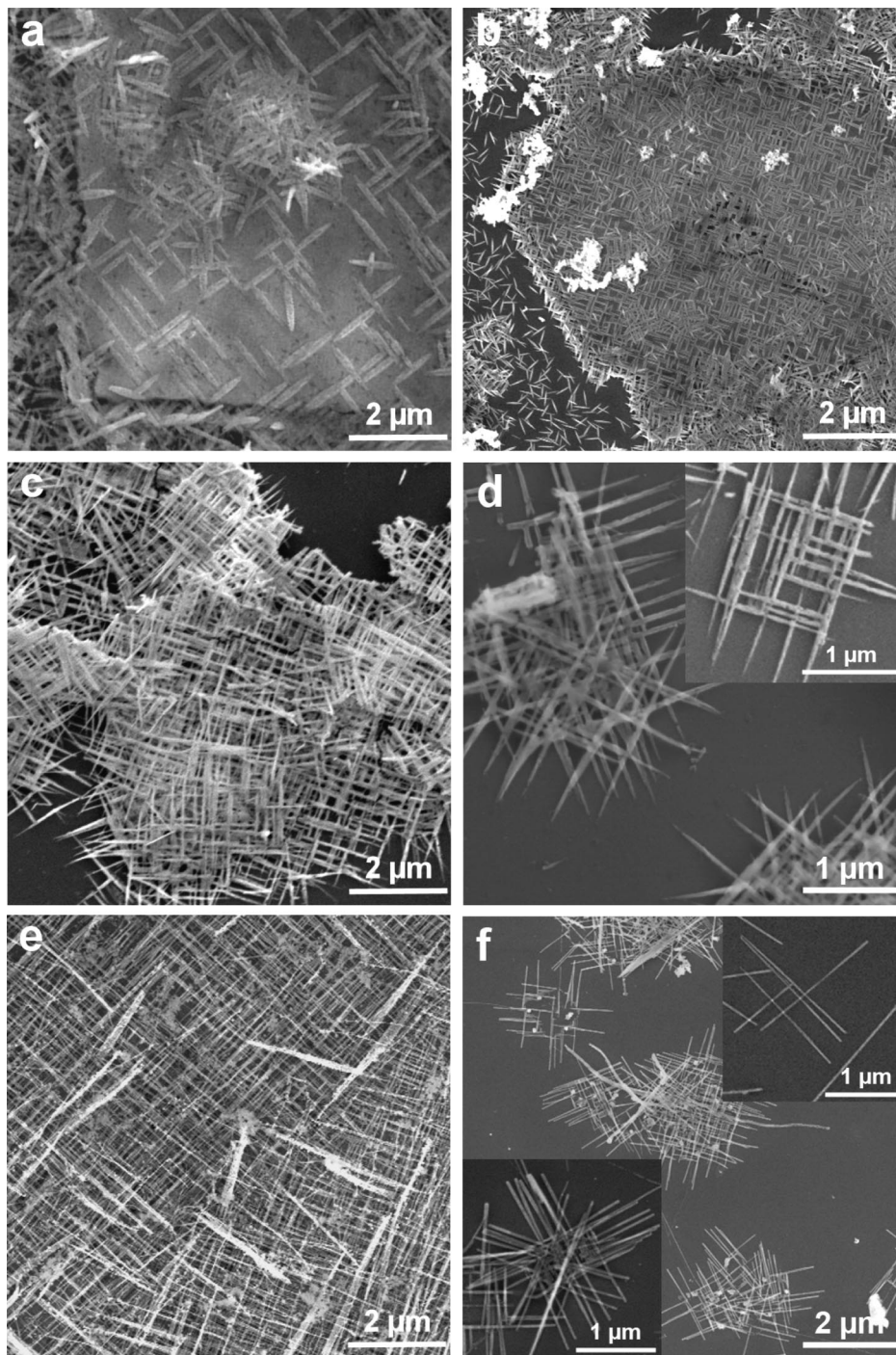


Figure 4. SEM images of CdS SGP-NWNs obtained with a reaction temperature of 185 °C for (a) 3 h, (b) 6 h, (c, d) 24 h, and (e, f) 48 h. Insert image in (d) is a typical monolayer SGP-NWN. Insert images in (f) are monolayer SGP-NWN (top right corner) and double-layer SGP-NWN (bottom left corner).

of the central area of the flake. When the reaction time was increased to 24 h, multilayer SGP-NWNs of high density were formed on the substrate (see Figure 4c). Figure 4d reveals a stack of SGP-NWN layers where the nanowires were aligned along different directions. The inset image in Figure 4d illustrates a typical monolayer SGP-NWN. The diameters of the nanowires are uniform and the tips are thinner than the bodies of the nanowires. When the reaction time reached 48 h, multilayer nanowire networks with high yield and fine uniformity were formed, as shown in Figure 4e. SEM images in Figure 4f further demonstrate the superposition and the alignment of the multilayer nanowire

networks. The inset on the bottom left corner of Figure 4f shows that the two-layer SGP-NWNs are aligned in two different directions while the inset on the top right corner of Figure 4f shows that the diameter of the nanowires is typically 40–50 nm. Both Figure 4e and Figure 4f show that the nanowires in the monolayer and multilayer SGP-NWNs are straight and uniform. They are no longer associated with the BiI₃ flakes.

The samples prepared at 185 °C with different reaction times were further characterized by the TEM technique. Figure 5a is a TEM image of a sample generated with a 3 h reaction time. It indicates clearly that nanowires formed on

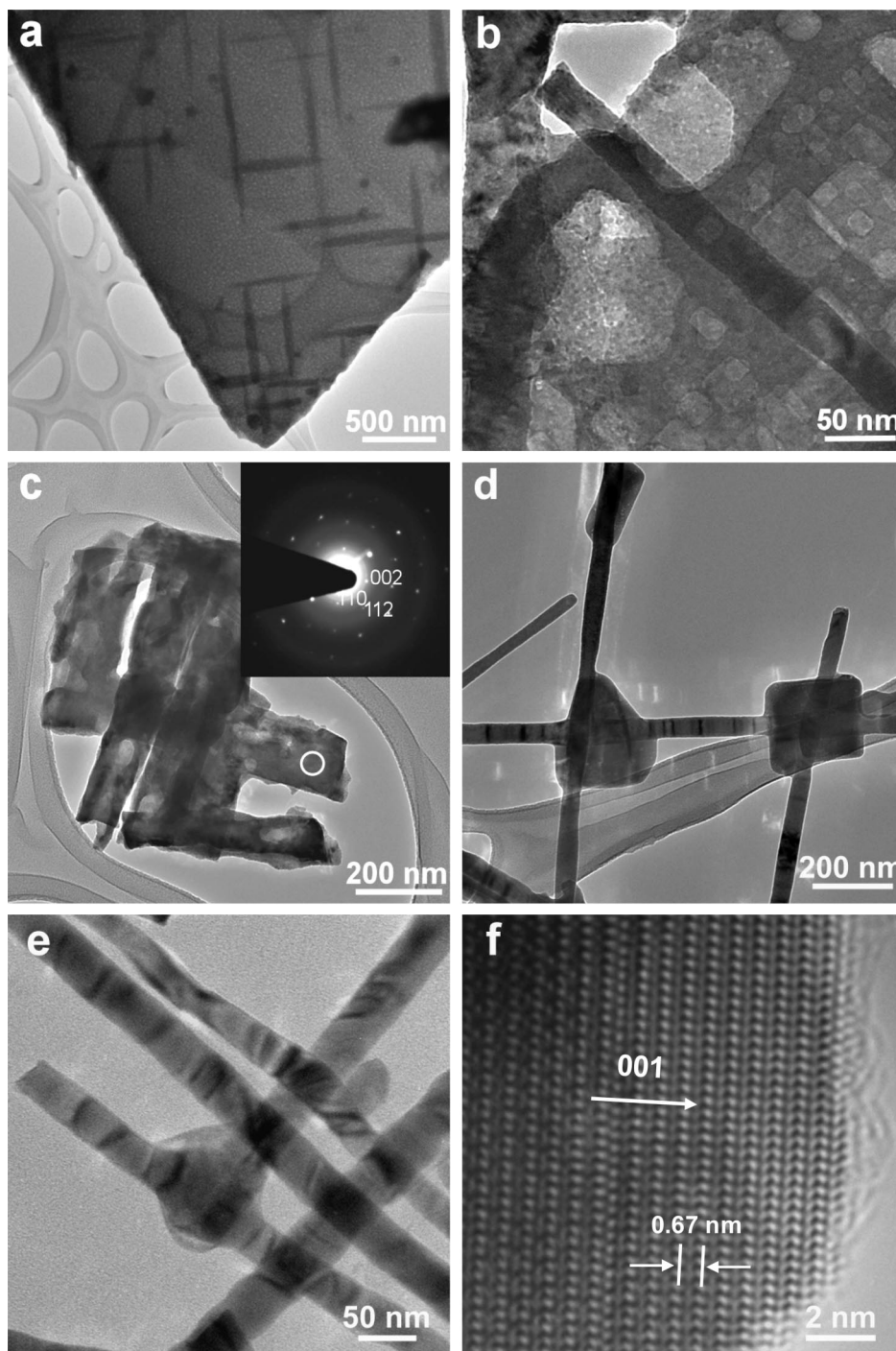


Figure 5. TEM images of SGP-NWNs grown at 185 °C for (a) 3 h, (b) 6 h, (c) 18 h, (d) 36 h, and (e) 48 h. Inserted in (c) is a selected area diffraction pattern (SAD) of the indicated region; (f) HRTEM image obtained from the tip of the nanowire on the CdS SGP-NWNs.

the surface of a BiI_x ($x=0-3$) flake. Figure 5b shows an image of a sample prepared with a 6 h reaction time. It reveals that a CdS nanowire with a diameter of 40 nm is lying on the surface of the flake. The thickness of the BiI_x flake, however, becomes thinner in some areas in comparison to the flake in Figure 5a. This suggests that the BiI_x flake gradually decomposed as the reaction time increased. Figure 5c displays a network fragment formed with an 18 h reaction time. A selected area diffraction pattern (SADP) confirms that the CdS nanowire grew along the [001] direction and was covered with residual BiI_x flakes (see inset in Figure

5c). We also found that, during the decomposition of BiI_x flakes, the cross points of the CdS SGP-NWNs are the areas where the residual BiI_x flakes were decomposed last in comparison to those attached to the body of the nanowires. (See Figure 5d. This sample was made with a 36 h reaction time.) For the sample prepared with a 48 h reaction time, the BiI_x flakes were almost completely decomposed from the CdS SGP-NWNs (see Figure 5e). A high-resolution TEM image (see Figure 5f) taken from the tip of the nanowire on the CdS SGP-NWNs further confirms that the growth is along the [001] orientation.

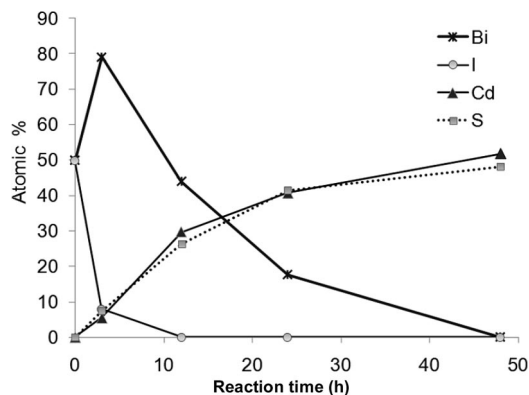


Figure 6. A plot shows the chemical composition change of the samples synthesized at 185 °C as a function of reaction time. The percentage content of Bi, I, Cd, and S is plotted using dark crosses, gray dots, dark triangles, and gray squares, respectively.

Energy-dispersive X-ray (EDX) spectroscopy was used to characterize the chemical composition of each sample. Due to the figure limitation in the text, the EDX spectra corresponding to each sample are shown in the Supporting Information (see Figure S1). A detailed analysis of the EDX spectra suggests that the percentage of Bi and I elemental compositions in a CdS SGP-NWN decrease as the reaction times increase. The atomic percent of the Cd and S chemical composition in the sample increases correspondingly, as depicted in Figure 6. Obviously, the decrease of the atomic percentage for the element I and Bi in the sample is due to the further decomposition of the BiI_x ($x = 0-3$) as the reaction time extends. When most of the I was evaporated during the BiI_x decomposition, the residual Bi seemed to react with S to form Bi_2S_3 particles in the solution. This is why the disappearance of the Bi seems slower (see Figure 6). A systematic evaluation of various SEM and TEM images and the EDX spectra suggests that CdS nanowires formed on the surface of the BiI_x flakes during the initial growth period while the formation of CdS SGP-NWNs was in conjunction with the BiI_3 flake decomposition.

Advantages of the CDE Synthesis and the Formation Mechanism of the SGP-NWNs. We have demonstrated the synthesis of monolayer and multilayer CdS SGP-NWNs using $\text{Cd}(\text{Ac})_2 \cdot 2\text{H}_2\text{O}/\text{S}/\text{C}_{32}\text{H}_{66}$ and BiI_3 flakes by a low-temperature (185 °C) chemical solution reaction. This procedure has many advantages in comparison to the high-temperature thermal processes for synthesizing CdS nanowires, branched nanowires, and nanorod heterostructures which are randomly grown on the substrates.^{23,24} Although some studies have shown the high-temperature epitaxial growth of nanostructures along the surface of the substrates,^{25,26} no nanowire network growth has been reported. Both methods, however, are highly substrate-dependent and require a high-temperature process to align nanowires. In our procedure, we chose a characteristic layered compound, BiI_3 with a rhombohedral structure, to achieve nanowire network forma-

tion. The procedure takes advantage of the fact that the BiI_3 thin flakes are bonded by the weak van der Waals forces between two adjacent structural layers.²⁷ The BiI_3 flakes with ordered polar Bi–I bonds on their surface provide a uniform 2D reaction interface and a dissolvable 2D template. By proper selection of the reaction temperature and the nanowire precursor, uniform and high-yield nanowire networks are formed and the BiI_3 2D templates are dissolved. This process not only is independent of the substrates used but also occurs at much lower temperatures.

Our experiments on the effects of reaction temperature (160–220 °C) and reaction time (3–48 h) demonstrate that the formation of the CdS SGP-NWNs has gone through the following processes: As indicated in Figure 2, the CdS nanoparticles with pyramid shape were first formed on the surface of BiI_3 flake. As the reaction temperature and time increase, these particles evolve into short CdS nanowires and finally assemble into the CdS SGP-NWNs (see Figure 4). Our study suggests that a CDE growth mechanism (comprised of three periods: chelation, deposition, and epitaxial elongation) is suitable for explaining the reaction. Due to the polar Bi–I and the bonding match between BiI_3 and CdI_2 ,^{28,29} the Cd^{2+} is chelated on the surface of BiI_3 flakes and forms the Bi–I–Cd layered structure at the interface between BiI_3 and the neutral $\text{C}_{32}\text{H}_{66}$. S is coordinated on the layer of Cd^{2+} due to electrostatic forces, resulting in a stable Bi–I–Cd–S layer structure after the $\text{CH}_3\text{COO}-\text{Cd}$ bond is decomposed. The next period is dominated by a deposition process. The CdS particles start to develop into short nanowires with continued deposition of Cd^{2+} and S. These nanowires continue to grow toward the edge of the flake by epitaxial elongation as the reaction time increases. Our results suggest that the CdS particle isotropic growth and the electrostatic force of the Bi–I layer play critical roles in the formation of the CdS SGP-NWNs.

Further experimental evidence indicates that the formation of CdS SGP-NWNs occurs at a reaction temperature between 160 and 185 °C. As shown in Figure 2, at 160 °C, the borders of the pyramid-shaped nanoparticles form in two intercrossed directions on the same flake. This nucleation is rationalized by four wurtzite domains connected to each other through twin boundaries on the BiI_3 flake. The alignment of pyramid-shaped crystalline nanoparticles is attributed to their lattice match with those of BiI_3 flakes. When the reaction temperature increases to 185 °C, T-shape intercrossed nanowires form on the surface of the BiI_3 flakes. This can be attributed to the coordination between multipod (bipod, tripod, and tetrapod) nanostructure growth and the electrostatic force of the Bi–I bonds. These nanostructures will elongate and interconnect to form SGP-NWNs assisted by the 2D template of the BiI_3 flake. As the highly ordered pyramid-shaped crystalline CdS nanoparticles continue to grow on the BiI_3 flake, they form ordered nanowires.

(23) Shen, G. Z.; Lee, C. *Cryst. Growth Des.* **2005**, *5*, 1085.

(24) Dong, L. F.; Gushtyuk, T.; Jiao, J. *J. Phys. Chem. B* **2004**, *108*, 1617.

(25) Sohn, J. I.; Joo, H. J.; Porter, A. E.; Choi, C.-J.; Kim, K.; Kang, D. J.; Welland, M. E. *Nano Lett.* **2007**, *7*, 1570.

(26) Hsin, C. L.; He, J. H.; Lee, C. Y.; Wu, W. W.; Yeh, P. H.; Chen, L. J.; Wang, Z. L. *Nano Lett.* **2007**, *7*, 1799.

(27) Nason, D.; Keller, L. *J. Cryst. Growth* **1995**, *156*, 221.

(28) Kondo, S.; Kato, A.; Saito, T. *Phys. Status Solidi A* **2000**, *182*, 661.

(29) Kim, D.; Karasawa, T.; Akai, I.; Komatsu, T.; Kobayashi, T. *J. Lumin.* **1996**, *66&67*, 443.

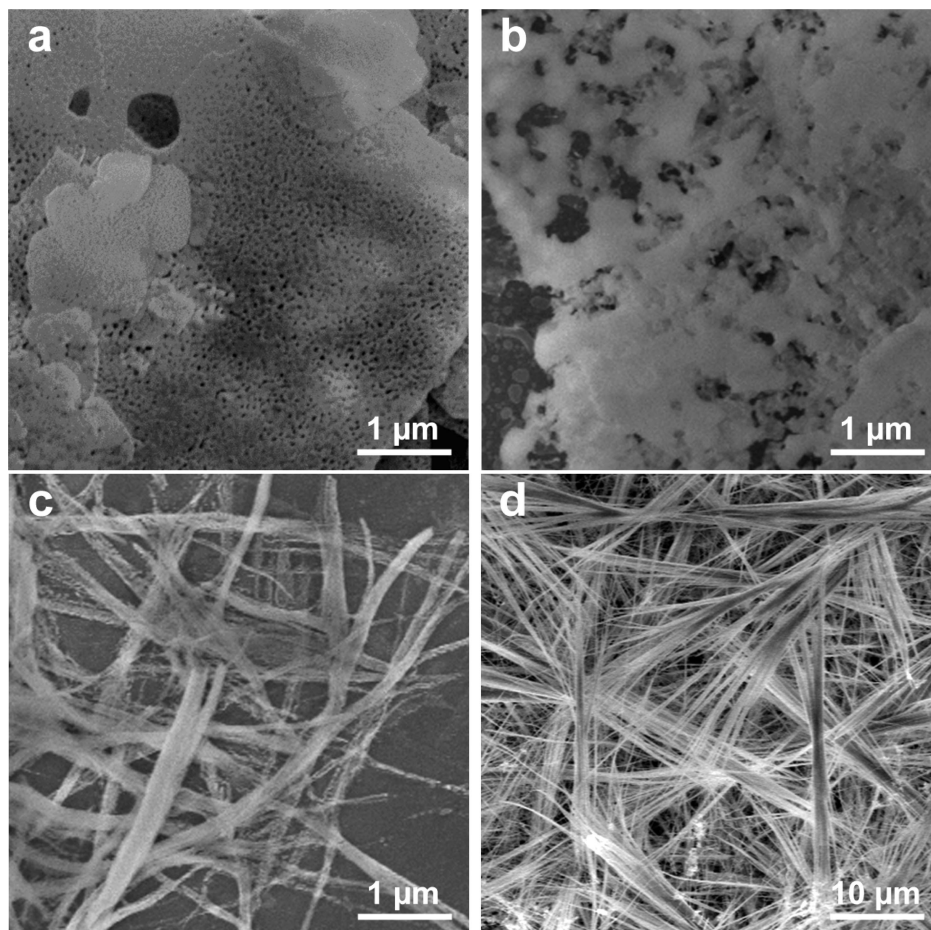


Figure 7. SEM images of samples obtained from the reaction without the addition of $\text{Cd}(\text{CH}_3\text{COO})_2$ at 185°C corresponding to the reaction times (a) 12 h, (b) 24 h, and (c) 48 h. Figure 7d shows a SEM image of BiS_x sheaf bundles formed from the reaction at 185°C for 48 h with the introduction of a large amount of BiI_3 flakes but without adding $\text{Cd}(\text{CH}_3\text{COO})_2$. TEM images and EDX spectra of the samples shown in (c) and (d) are presented in the Supporting Information.

We also noted that some nanosheets with square dents were formed during the reaction (Figure 5b). To further clarify the formation of the ordered nanostructure, the extended reactions without adding $\text{Cd}(\text{CH}_3\text{COO})_2 \cdot 2\text{H}_2\text{O}$ were conducted. As-synthesized products display a series of morphologies from porous BiS_x films to perpendicularly interconnected porous BiS_x nanowires corresponding to different reaction times. These BiS_x nanostructures are shown in Figure 7a–c. More results are shown in the Supporting Information (Figure S2a). These results suggest that the nanosheet with square dents are caused by both the decomposition of the BiI_3 flake and the deposition of Cd^{2+} or Bi^{3+} cations and results in the alignment of CdS nanowires or porous BiS_x nanowires. In another experiment, a large amount of BiI_3 flakes was introduced into the reactions without adding $\text{Cd}(\text{CH}_3\text{COO})_2 \cdot 2\text{H}_2\text{O}$. The purpose of this experiment is to investigate the effect of BiI_3 flakes on the formation of Bi_2S_3 growth. The results show that only high-yield BiS_x sheaf bundles (Figure 7c) were obtained due to the crystal splitting as reported by Tang and Alivisatos.³⁰ This confirms that the perpendicularly interconnected porous BiS_x nanowires were formed by the deposition of Bi^{3+} and S on the BiI_x flake with square dents. As stated in this report, when we introduce both BiI_3 flakes and $\text{Cd}(\text{CH}_3\text{COO})_2 \cdot 2\text{H}_2\text{O}$

into the reaction, it leads to the formation of the CdS SGP-NWNs. Our EDX chemical analysis demonstrates that these SGP-NWNs consist of Cd and S instead of Bi and S.

Our other experiments reveal that reaction parameters used to synthesize monolayer CdS SGP-NWNs can be used to synthesize multilayer CdS SGP-NWNs as well. Reaction happens on each layer of the BiI_3 flakes if enough Cd^{2+} and S are used. We also synthesized several vertically aligned CdS SGP-NWNs based on the vertically aligned BiI_3 flakes on the substrate (see Figure S3). This suggests that it is possible to fabricate CdS SGP-NWNs on different layers of flakes with different aligning orientations.

Further investigation also demonstrates that the CDE low-temperature chemical procedure can be used to synthesize other types of nanowire networks. For example, the CdSe SGP-NWNs have also been successfully synthesized on Si, SiO_2/Si , and glass substrates (see Figure S4).

Conclusions

A one-step low-temperature chemical procedure with the assistance of the BiI_3 flakes to synthesize CdS SGP-NWNs in $\text{Cd}(\text{Ac})_2 \cdot 2\text{H}_2\text{O}/\text{S}/\text{C}_{32}\text{H}_{66}$ was developed. The formation of the SGP-NWNs was believed to follow a CDE growth mechanism. A series of experiments demonstrates that using BiI_3 flakes and nanostructure precursors enable the synthesis

(30) Tang, J.; Alivisatos, A. P. *Nano Lett.* **2006**, *6*, 2701.

and assembly of nanostructure networks in one process. This provides great opportunities for fabricating large-scale integrated nanoelectronics and optical nanodevices.

Acknowledgment. This work is supported by the National Science Foundation under the grants of ECCS-0217061, ECCS-0348277, and ECCS-0520891.

Supporting Information Available: Energy-dispersive X-ray (EDX) spectra and corresponding images of the samples synthesized

with different reaction temperatures and times; TEM images and EDX spectra of BiS_x nanostructures synthesized with different reaction times without $\text{Cd}(\text{CH}_3\text{COO})_2 \cdot 2\text{H}_2\text{O}$; SEM images of the standing CdS SGP-NWNs and the CdSe nanowire networks (PDF). This material is available free of charge via the Internet at <http://pubs.acs.org>.

CM800887Z